Investigation of Electrospun Fiber Diameter Distribution and Process Dynamics

Xuri Yan, Michael Gevelber

***Abstract*—Electrospinning employs electrostatic force to draw and accelerate a jet of charged polymer solution or melt from a nozzle placed in electric field. This fiber solidifies and deposits on a grounded collector forming a nonwoven fiber mat. One of the most important quantities related with the emerging applications of electrospun fibers is the fiber diameter. However, the current state-of-the-art electrospinning process results in unpredictable and time varying diameter distributions.**

This work is focused on developing a better understanding of the relation between the process physics and the resulting fiber diameter characteristics. A well instrumented and computer based measurement and actuation system has been developed for facilitating the study. The relation of the electric field and induced charge density to the process states and fiber diameter are studied. The correlation between the variation of some measured variables and the resulting fiber diameter distribution is investigated.

***Index Terms*—electrospinning, nanofiber, charge density, process control**

I. Introduction

ELECTROSPINNING uses an external electrostatic field to stretch and accelerate a charged polymer solution or melt jet and is capable of producing a nonwoven fabric of submicron fibers. There has been a considerable growth and development in electrospun fibers for both research activity and commercial fabrication due to the ease with which nanometer scale fibers can be produced from both natural and synthetic polymers.

Generally, in this process, a syringe pump is used for controlling the polymer liquid flow rate and delivering the liquid to a small diameter nozzle (Fig. 1). A high-voltage power supply generates an external electrical field between the nozzle and a grounded collector placed some distance from the nozzle. The interaction of the electrostatic forces of the surface charge and the surface tension of the liquid causes a "Taylor" cone to form on the tip of the nozzle. When the charge breaks a threshold level and overcomes the surface tension, a straight jet is ejected from the apex of Taylor cone. This jet remains straight for some distance until a critical point where a variety of forces cause it to "bend" or "whip". Meanwhile, solvent is evaporated as the jet flies to the collector. Ultimately, a non-woven fiber mat is formed on the collector. The electrospun fiber size can be two to three orders of magnitude smaller than conventional commercial fibers.

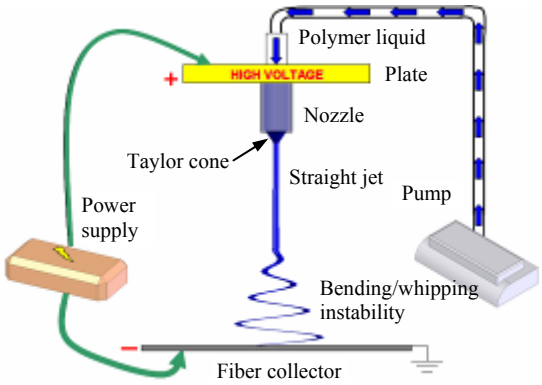

Fig. 1. Schematic of electrospinning setup

Though the unique features of electrospun fibers make them a very exciting technology for a number of applications, the current electrospinning process results in unpredictable and time varying diameter distributions which limit many advanced emerging applications. Therefore, it is critical in many applications for the specified diameter distributions to be manufactured reliably and robustly. In order to deliver more accurate control of fiber diameter, we need to develop a better description of the process dynamics in terms of the impact of variation sources and the relationship between measured variables and process states to fiber diameters. To achieve this objective, an integrated electrospinning measurement and actuation system was developed which provided not only a basic electrospinning apparatus, but also the capability of monitoring multiple process states in real-time and controlling the actuators of the syringe pump and high voltage power supply.

The real-time measurements of the Taylor cone volume (or the upper jet diameter), electric current, and charge density provide a useful basis for selecting an appropriate operating regime. Moreover, the real-time data of these measured variables can be used to quantitatively characterize the process variations. The results of this work help the development of appropriate control strategies for achieving consistent and controllable fiber diameters and process.

Manuscript received April 17, 2009. This work was supported by NSF under Grant CMMI 0826106.

Xuri Yan is with Boston University, Boston, MA 02215 USA. (e-mail: xryan@bu.edu).

Michael Gevelber is with Boston University, Boston, MA 02215 USA. (e-mail: gevelber@bu.edu).

II. Experimental Procedure

A. Materials

Polyethylene oxide (PEO, molecular weight, $M_w = 4\times10^5$ and 2×10^6) powders purchased from Aldrich were used to prepare solutions that were used as the working fluids. Different molecular weight PEO was dissolved in deionized water solvent which was pre-heated to 40 °C at different concentrations. All solutions were stored in a refrigerator at 5 °C and all experiments were conducted at 25 °C in air.

B. Fiber dimension characterization

Fibers were collected on an aluminum foil sheet. Fiber images were obtained by FESEM (Field Emission Scanning Electron Microscope, Zeiss SUPRA 40VP). 5-8 samples were cut from each sheet to obtain the SEM images with 5 images taken per area. With approximately 10-15 fibers per image these were typically on the order of 300 to 500 fibers measured. This provided a sufficient data set for obtaining a diameter distribution histogram. In order to assist in collecting this data, The software shown in Fig. 2 was developed based on the LabView imaging analysis module to assist in collecting, analyzing, and plotting histograms of fiber size distribution. Each fiber was measured 5-10 times along its length and then an average was calculated automatically for precision. The software also automatically numbers the fibers measured and catalogs both the diameter values and fiber numbers in the original image to track the measurement record process.

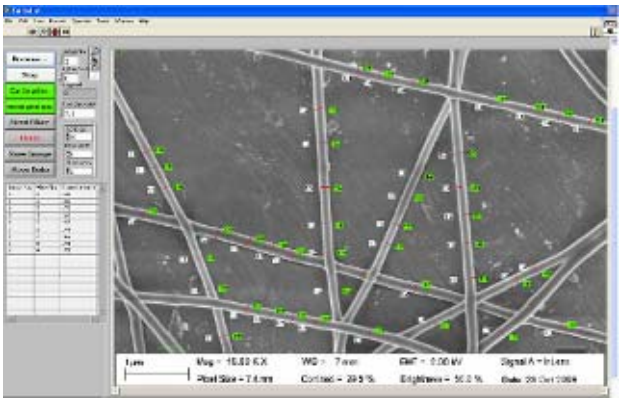

Fig. 2. The interface of the software developed for fiber dimension analysis from SEM images

III. Development of Measurement and Actuation System

The electrospinning test-bed consists of an upper aluminum disk with diameter of 15cm and an aluminum collector with a size of 30cm by 30cm set up in a plexiglass enclosure with a variable offset distance. It is noted that in this study, this distance was fixed at 35cm for all experiments, unless otherwise indicated. The electrospun fibers are collected on this large flat aluminum collector.

A stainless steel needle (or nozzle) with inner diameter of 1 millimeter and outer diameter of 1.6 millimeters was inserted through a hole in the center of the upper disk, protruding 10 millimeters out from the disk. A digital syringe pump (Harvard Apparatus, PHD 2000) delivers the fluid from this syringe to the needle and controls the flow rate. A high voltage power supply (Gamma High Voltage Research, XRM30P) was connected to the upper disk and needle to provide up to 30,000 volts of driving potential relative to the grounded collector. Both the actuators (power supply and pump) have input/output capabilities for interfacing with a computer for real-time data acquisition and control. Not only the command signals, but also the actual input values are monitored.

Two video cameras are integrated into a LabView-based image acquisition and real-time processing software to obtain the corresponding information regarding the Taylor cone, straight jet, and bending instability regions. Fig. 3 shows a schematic for the real-time measurements, including the variables: Taylor cone volume, $\forall$, the straight jet diameter, d_{jet}, the length of the straight jet, L, and the angle θ of the whipping region. In addition, the jet current, I, is measured by a current sensor and recorded simultaneously. Jet current can be used to estimate the charge density carried by the jet surface and the resulting electric force.

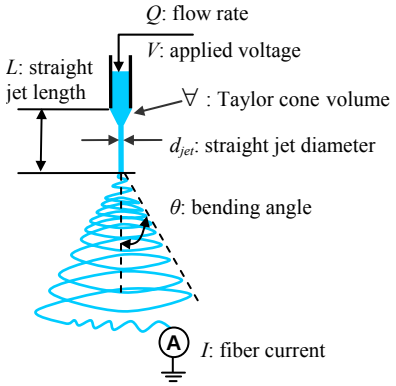

Fig. 3. Measurable variables for electrospinning process

The 1st camera used in this system is an ISG CMOS camera with resolution of 2048×1536 pixels. It is used with a Nikon 70-300mm macro lens to acquire images of the Taylor cone and upper jet region at the rate of 20 frames per second (fps). The back lighting system includes a MD 150 fiber light and a sandblasted glass diffuser from Edmund to provide sharp edge contrast for this vision system and guarantees precise measurements. The exposure time is usually set to 0.02 seconds.

Fig. 4(A) shows the image of Taylor cone & upper jet region. The dashed square with length L_{tc} defines the region within which the Taylor cone volume $\forall$ is obtained. It is noted that the length, L_{tc}, is not the actual length of the Taylor cone. For a given solution, the shape and size of the Taylor cone are determined by electric field strength and flow rate. With the needle used in current setup, the Taylor cone length is about 1-3mm which increases with flow rate and decreases with electric field.

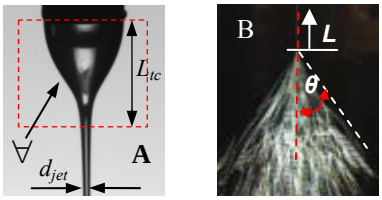

Fig. 4. Real-time measurements of electrospinning process
A). Taylor cone & upper jet; dashed square shows the region with length L_{tc} for obtaining ∀
B). Bending angle, θ and straight jet length, L

Each image is scanned by the software from top to bottom automatically and a series of diameters are obtained through edge detection. With these diameter values, the Taylor cone volume, ∀ , can be computed by the sum of a series of truncated cone volumes.

The straight jet diameter, d_{jet}, is measured at the location where it is close to the bottom of the field of view by the 1st camera as shown in Fig. 4(A).

The 2nd camera (Basler A602f) is used to obtain the straight jet length, L, the angle, θ, of the bending envelope cone (Fig. 4(B)). Front light is used for this camera. The straight jet length is defined as the distance between the needle tip and the onset of bending.

A current sensor was developed to measure the extremely small electric fiber current. It is basically an amplifier which outputs a zero to 10 volts analog signal. This current sensor is placed between the collector and the NI USB-6008 data acquisition (DAQ) card. The voltage signal is sampled by this DAQ device at 1000 Hz, and correlated to image data.

IV. Results and Discussion

A. Quantitative characterization of process dynamic variations

The changing of Taylor cone shape with voltage, and the minimal voltage or electric field strength for a stable jet has been observed by many researches. However, quantitatively characterizing the process variations in terms of the Taylor cone shape/volume, jet diameter, electric current, as well as charge density is not established.

2.5wt% aqueous PEO solutions (M_w=2,000,000) was used in this set of experiments. The length, L_{tc}, for obtaining Taylor cone volume was fixed at 2.8mm. The plate separation distance, H, was set to 35 cm in order to get dry fibers. All of the applied voltages, V, could be normalized by this distance and expressed as electric fields, $E_\infty = V/H$. The flow rate was set to Q=0.01ml/min and then the applied voltage was varied from low to high to explore the operating conditions and variations.

The standard deviation of the real-time measured data normalized by their average which is denoted by σ^N is used to characterize the dynamic variations.

Fig. 5 shows the real-time measurement of volume, ∀ and its photograph of the operating condition of 13.7kv. With this low voltage condition, the volume has significant fluctuations. σ^N in terms of percentage is used to characterize the magnitude of this fluctuation. In this case, the σ^N is as large as 14.2%.

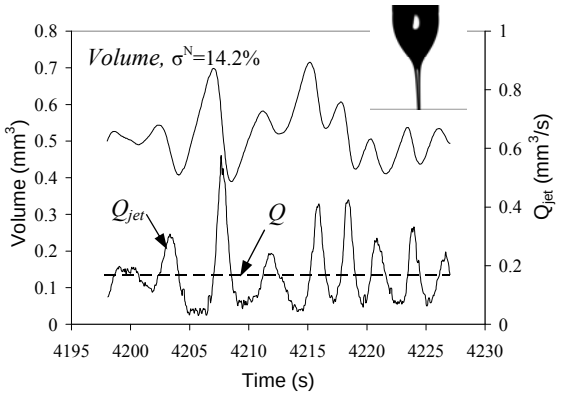

Fig. 5. Dynamic volume and Q_{jet} of the condition V=13.7kv and Q=0.01ml/min (0.167mm³/s), and the corresponding Taylor cone image

B. Characterization of dynamic flow rate and charge density

The fixed value of L_{tc} in Fig. 4(A) provides the basis for comparing the Taylor cone shapes of different operating conditions, since with constant L_{tc}, the changes in ∀ reflects the changes in the Taylor cone diameter and shape. Moreover, the specific region defined by L_{tc} functions as a control volume for mass conservation analysis. The actual dynamic flow rate that flows into the downstream region, Q_{jet}, can be obtained from the dynamic change of ∀ and the pump supply flow rate Q by the following equation:

$$Q_{jet}(t) = Q - \frac{d\forall(t)}{dt} \qquad (1)$$

The Taylor cone volume, ∀ , is modeled as a mass capacitor here. This relation is illustrated in Fig. 6.

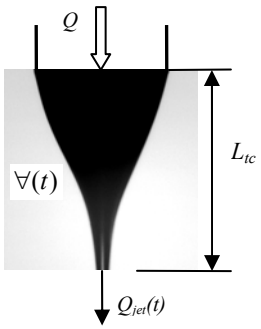

Fig. 6. Dynamic jet flow rate at the exit of the control volume with length L_{tc}

Fig. 5 shows both the dynamic jet flow rate, Q_{jet}, of 13.7kv derived from (1) and the pump flow rate Q=0.01ml/min≈0.167mm³/s. It is observed that the flow rate, Q, is significantly different with the actual flow rate in the downstream, Q_{jet}, if large fluctuations exist in upstream region. Therefore, Q_{jet} is a much more accurate estimation of the actual

downstream flow rate at a given instant than the pump flow rate, Q, in the region where solvent evaporation is insignificant.

Numerous researchers reported that the charge density is one of the most important parameters which determine fiber size. The dynamic volumetric charge density is calculated by using (2).

$$\rho_e(t) = I(t) \Big/ Q_{jet}(t) \qquad (2)$$

Equation (2) is valid only when both the solvent evaporation and the conduction of electric current are negligible. Thus, ρ_e is used as the initial volume charge density carried by the electrospun jet in present work.

Fig. 7 shows the dynamic electric current and the corresponding dynamic volumetric charge density derived from (2) for the experiment shown in Fig. 5. It is observed that the large fluctuations in volume result in large fluctuations in jet flow rate, Q_{jet}, and consequentially cause the fluctuations in current, I, and charge density, I/Q_{jet} downstream. It shows that measuring the dynamic volume by real-time photography technology is necessary for estimating the actual dynamic flow rate, electric current, and charge density.

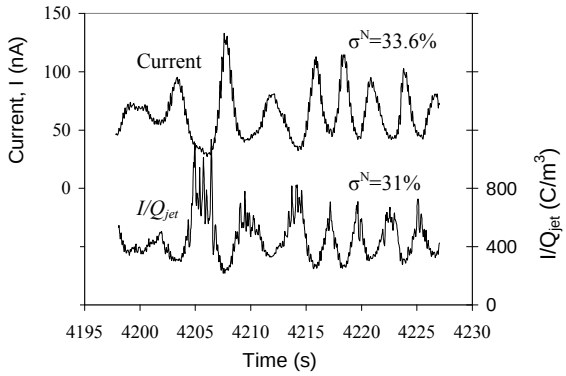

Fig. 7. Dynamic current and I/Q_{jet} of the condition V=13.7kv, and Q=0.01ml/min

C. Determination of the operating regime with minimal jet fluctuations

Fig. 8 plots the normalized standard deviation (σ^N) of Taylor cone volume as a function of voltage for the same solution used in section A and B. The results show that either when voltage is lower than 14.3kv or when voltage is higher than 16kv, the σ^N will increase significantly. On the contrary, operating within the range from 14.3kv to 16kv, the dynamic volume data result in much smaller σ^N, which in this case is smaller than 5%.

For the low voltage condition of 13.7kv, large magnitude, periodic variations exists in Taylor cone volume and other measured variables shown in Fig. 5 and Fig. 7. Theron *et al.* also observed these fluctuations in their work [1]. The competition between supply of the solution by the pump and its withdrawal caused by the electric field leads to the change in shape and volume of the Taylor cone region.

When electric field strength was further increased, the cone shapes became more tapered and even less variations were observed. Fig. 9 shows if the process is preformed in the minimal jet fluctuation regime, the fluctuation magnitudes of the Taylor cone volume and current are significantly decreased.

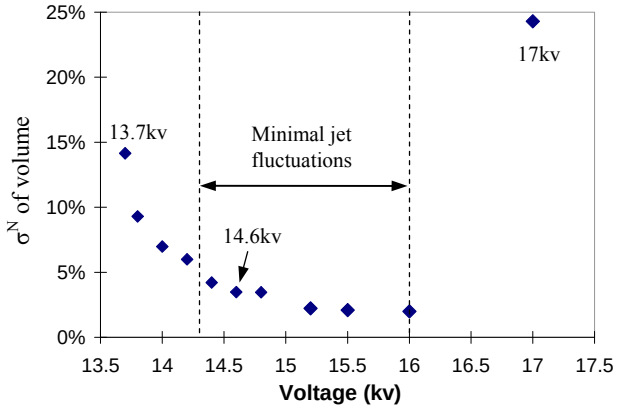

Fig. 8. The normalized standard deviation of volume variations as a function of voltage, and the minimal jet fluctuation regime for Q=0.01ml/min of the solution used

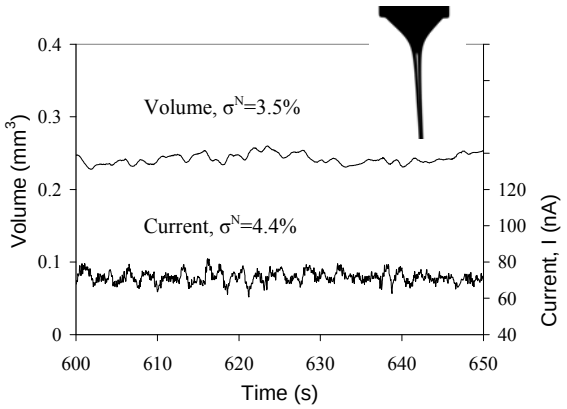

Fig. 9. Dynamic volume and current of the condition V=14.6kv and the corresponding Taylor cone image

When the electric field was increased above certain value, the Taylor cone was no longer observed as the image is shown in Fig. 10. The jet seemed to originate directly from the nozzle and sometimes it moved around the edge of the nozzle tip. Shin [2] and Deitzel [3] reported this phenomenon too. Increasing the voltage caused the rate at which solution was removed from the Taylor cone to exceed the rate of delivery of solution to the tip needed to maintain the conical shape of the surface.

Fig. 10 shows the dynamic plots of volume and current for the voltage condition, V=17kv, beyond the minimal jet fluctuation regime. The large periodic fluctuations in volume and current show up again.

The example shown in Fig. 10 does not mean that the process will undergo these large periodic fluctuations as long as the Taylor cone recedes into the nozzle. In contrast, sometimes the variations are still small even when there is no well defined Taylor cone at the tip of the nozzle due to the high voltage. However, for a long term run, the Taylor cone may move up

along the nozzle's inner wall due to the unbalance between the flow rates of supply and withdrawal. Therefore, it is not a desired operating regime for a stable and consistent spinning process. At this point, the imaging technology is necessary for selecting appropriate operating conditions, since sometimes it is difficult to know that the Taylor cone has recede into nozzle without the help of imaging system.

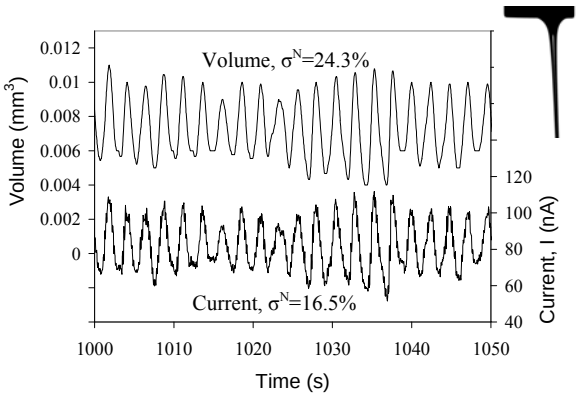

Fig. 10. Dynamic volume and current of the condition V=17kv and the corresponding Taylor cone image

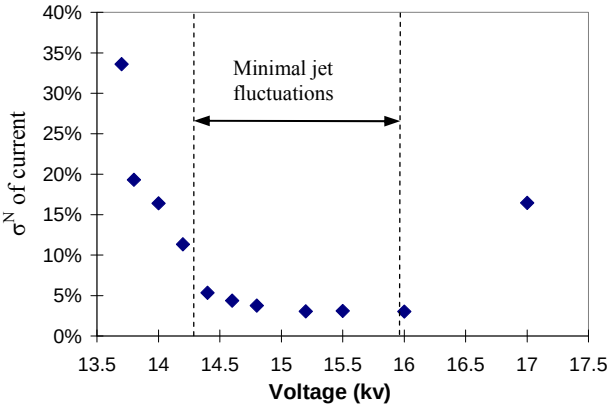

Fig. 11. The normalized standard deviation of current variations as a function of voltage, and the minimal jet fluctuation regime for Q=0.01ml/min of the solution used

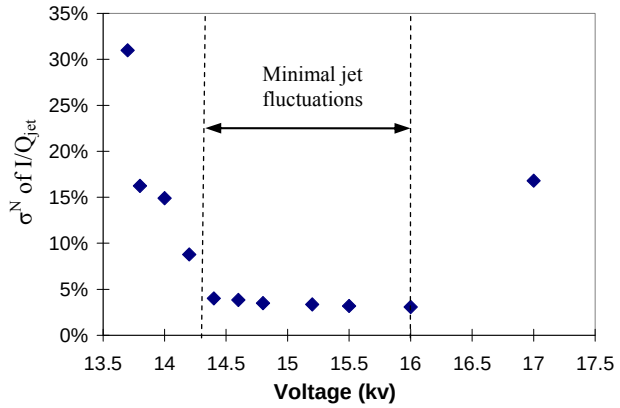

Fig. 12. The normalized standard deviation of volumetric charge density variations as a function of voltage, and the minimal jet fluctuation regime for Q=0.01ml/min of the solution used

Fig. 11 and Fig. 12 show the σ^N of the current and charge density as functions of voltage respectively for the conditions in Fig 8. Same as the results in Fig. 8, operating within the range from 14.3kv to 16kv, both the current and charge density result in much smaller σ^N.

D. Correlation between measured variables and fiber diameter distribution

To examine the impact of the upstream variations on fiber diameter as well as the relation of measured variables to fiber diameter distributions, the 7wt% aqueous PEO solutions ($M_w=4\times10^5$) was used. The minimal jet fluctuation regime was identified first and all the runs were performed within this regime. The resulting fiber diameter distributions were characterized by the normalized standard deviation, σ^N. Same experimental design as above sections, the distance (H) between the two plates was fixed at 35cm. For each experiment, the process was run for 3 to 5 minutes until there were enough fibers deposited on the aluminum foil sheet.

Fig. 13 summarizes the σ^N of the $\forall$, I, I/d_{jet}, as well as fiber diameter for 3 voltage conditions (25.5kv, 27.5kv, and 30kv). Their flow rates are all 0.05ml/min. These experiments indicate that several factors correlate with the trends of the resulting fiber diameter variation, as measured by the σ^N. The variations in Taylor cone volume, fiber current, and charge density are correlated to the resulting fiber diameter variations. The σ^N of both the measured variables and fiber diameter decrease as voltage increases within the minimal jet fluctuations regime. The mean of the fiber diameter decreases as voltage increases as well.

Fig. 14 and 15 show the corresponding SEM images and fiber diameter histograms for the 3 runs in Fig. 13. 40 SEM images were taken and more than 500 fibers were measured for each run in order to collect sufficient data for fiber diameter distribution. For the low voltage run of V=25.5kv, the large variations are seen in both the SEM image (Fig. 14) and the histogram (Fig. 15). In contrast, for the high voltage run of V=30kv, much smaller variations are observed in both the SEM image and the diameter histogram which correspond to smaller σ^N in the measured variables shown in Fig. 13.

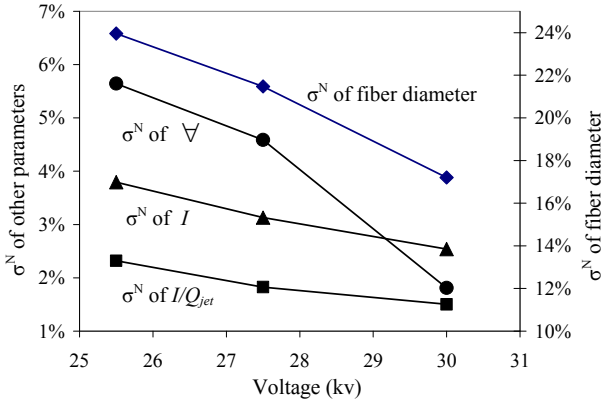

Fig. 13. Normalized standard deviations of 3 different voltage conditions for 7wt% PEO (Mw=400,000, Q=0.05ml/min)

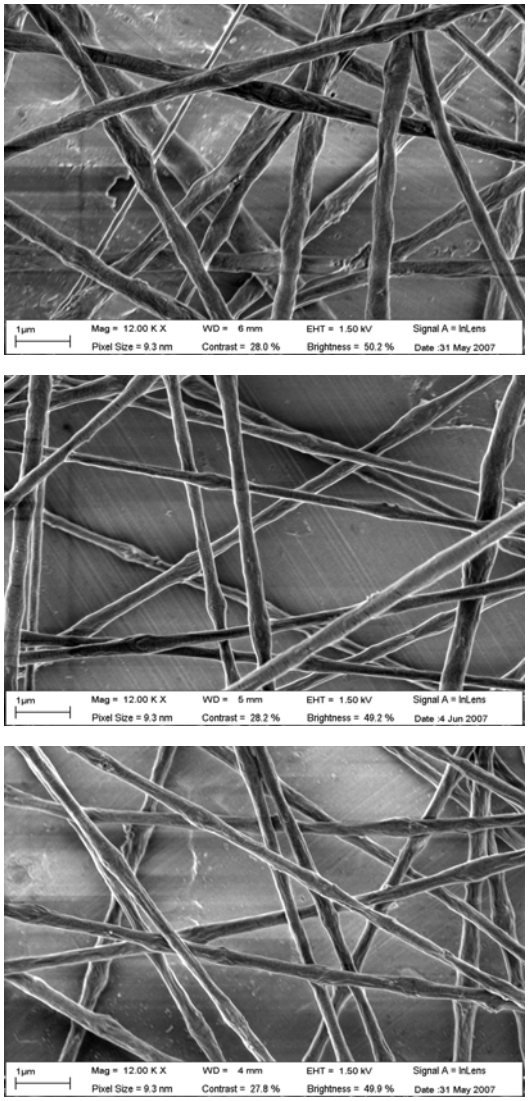

Fig. 14. SEM images of the voltage condition in Fig. 13: V=25.5kv (up); V=27.5kv (middle); V=30kv (low) (Q=0.05ml/min, scale bar=1μm)

Based on above investigation, it is found that the free boundary region, Taylor cone, is important since it determines the volumetric flow of material into the jet, which is one of the major factors that cause the downstream variations and determine the fiber diameter distributions.

These results suggest that reducing variations in the upstream region of the process could result in reduction in downstream variations. The observation also reveals that some of the variables measured correlate well with the resulting variations in fiber diameter. If the variations in charge density, Taylor cone volume, or current are reduced, the variations in fiber diameter will decrease too.

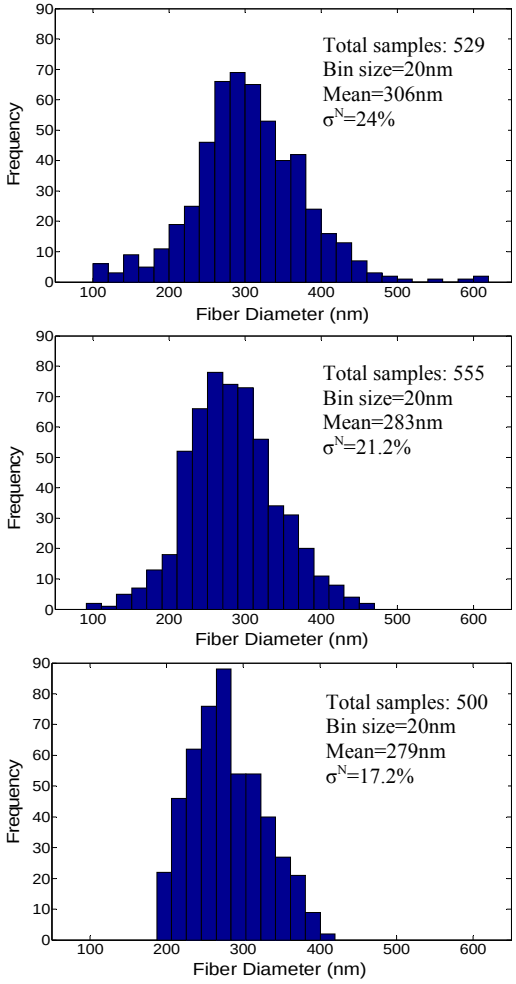

Fig. 15. Fiber diameter distributions for the voltage conditions in Fig. 13: V=25.5kv (up); V=27.5kv (middle); V=30kv (low) (Q=0.05ml/min)

E. Analysis process dynamics and the control implication

Fig. 16 shows the dynamic cone volume and electric current of the V=25.5kv condition in Fig. 13. Fig. 17 shows the resulting Fourier power spectral decomposition of these two critical variables in Fig. 16, Taylor cone volume and fiber current. Both plots reveal that there are dominant low frequency modes of variation (on the order of 1 Hz and less), which is possible to be compensated for by the adequate bandwidth of the power supply actuator for electrospinning. It suggests that there is a possibility to improve the performance of the electrospinning process by reducing the factors that cause diameter variations by using real-time control.

Low frequency fluctuations in Taylor cone and upper jet regimes are commonly observed. Theron *et al.* [1] observed this oscillation in their experiments and explained it by the competition between supply of the solution by the syringe pump and its withdrawal caused by the electric field.

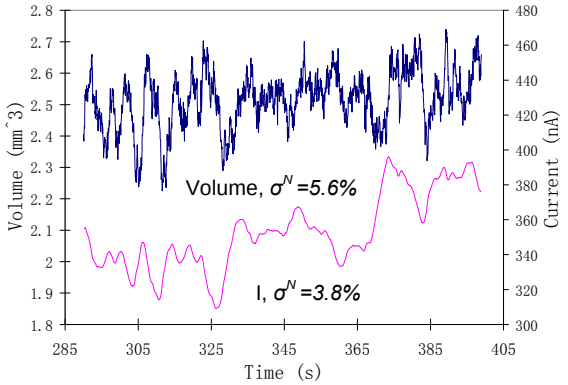

Fig. 16. Dynamic plots of the run with V=25.5kv and Q=0.05ml/min in Fig. 13

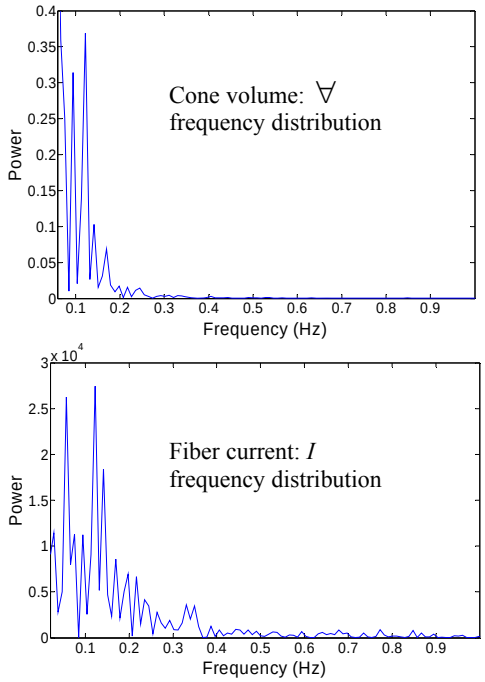

Fig. 17. Dominant frequency modes of dynamic volume (up) and current (low)

V. Conclusion

The use of a vision system and current sensor in this study provide the capability for measuring process variations and make it easy to map out the minimal jet fluctuation regime in terms of finding appropriate voltage set points. This system provided data to help develop a unique understanding of the input-output relation, process dynamics, and characteristic of variation of the electrospinning process.

The process dynamic variations were quantitatively characterized by the normalized standard deviation. It was found that the downstream portion of the electrospinning process is highly dependant upon the upstream portion of the process. The behavior and fluctuation in the Taylor cone and upper jet regions are highly influenced by electric field strength and charge density and have significant impacts on electrospun fibers. The results indicate that the variations in Taylor cone volume, fiber current, and charge density are correlated to the resulting fiber diameter distributions. Thus, control of the potential difference applied to match the flow rate in order to maintain a minimal fluctuation jet throughout the electrospinning process is necessary.

The analysis also shows that the voltage actuator could take effective control action with the required bandwidth. This work provides the basis for developing appropriate control strategies in order to reduce both the process variations from run-to-run and during a run.

References

[1] S.A. Theron, E. Zussman, A.L. Yarin, "Experimental investigation of the governing parameters in the electrospinning of polymer solutions", *Polymer,* vol. 45, pp. 2017–2030, 2004.

[2] Y.M. Shin, M.M. Hohman, M.P. Brenner, G.C. Rutledge, "Experimental Characterization of electrospinning: the electrically forced jets and instabilities" *Polymer*, vol. 42, pp. 9955, 2001.

[3] J.M. Deitzel, J. Kleinmeyer, D. Harris, N.C. Beck Tan, "The effect of processing variables on the morphology of electrospun nanofibers and textiles", *Polymer*, vol. 42, pp. 261–272, 2001